Available online at www.sciencedirect.com
SCIENCE DIRECT
Journal of Sound and Vibration 297 (2006) 215–226
JOURNAL OF SOUND AND VIBRATION
www.elsevier.com/locate/jsvi

Structural power flow analysis of Timoshenko beam with an open crack

X. Zhu, T.Y. Li*, Y. Zhao, J.X. Liu

Department of Naval Architecture & Ocean Engineering, Huazhong University of Science & Technology, Wuhan 430074, PR China

Received 9 May 2005; received in revised form 4 January 2006; accepted 27 March 2006
Available online 2 June 2006

Abstract

In this paper, the structural power flow characteristics of cracked Timoshenko beams are presented. The case of an infinite Timoshenko beam with an open crack is considered. The crack in the Timoshenko beam structure is modeled as a rotational spring with a constant flexibility which is deduced from the relationship between the strain energy and stress intensity factor in fracture mechanics. The flexural wave motions of perfect Timoshenko beam and cracked Timoshenko beam are investigated, then the input power flow and transmitted power flow of perfect and cracked beams are calculated. The results show that the vibrational power flow of cracked beam is highly related to the location and depth of the crack. Contours of input power flow with different frequencies are constructed to identify the location and depth of the crack. This method is very promising for the detection and location of structural damage in the future work.

1. Introduction

Due to different causes, cracks are always found in the element of a structure. In order to improve the safety and reliability of the structure, it is urgent to make early detection and locating of the cracks. For this reason many damage-detection methods are developed. Non-destructive evaluation methods, such as ultrasonic testing, X-ray, magnetic field methods, etc., are usually costly and time consuming for the large-scale structure. The modal-based damage identification methods are utilized widely in recent years. The basic idea is that the existence of a crack in a structure results in a reduction of stiffness which in turn produces a decrease in natural frequencies and changes in the modal parameters (mode shapes, modal damping, etc.). Therefore, changes in the physical properties of a structure will cause detectable changes in the modal properties. Though this method may have advantages, it possess a number of major disadvantages [1].

In the previous studies, many authors have developed different methods to detect the crack in the beam structure. Gounaris and Dimarogonas [2] have developed a finite element for a cracked prismatic beam for structural analysis based on the compliance matrix for the crack. Rizos et al. [3] considered the crack in beam as a local flexibility and developed a crack detective method by the measured vibration modes to determine the crack location and depth. Lele and Maiti [4] detected the location of crack in short beams based on frequency

*Corresponding author.
E-mail address: ltyz801@tom.com (T.Y. Li).

0022-460X/$ - see front matter © 2006 Elsevier Ltd. All rights reserved.
doi:10.1016/j.jsv.2006.03.034

measurements, taking into account the effects of shear deformation and rotational inertia and representing the crack by a rotational spring. Krawczuk et al. [5] introduced a finite spectral element of a cracked Timoshenko beam for modal and elastic wave propagation analysis. In Ref. [6], a method of crack detection in beam is provided by wavelet analysis of transient flexural wave, and the transient flexural wave propagation was calculated by the reverberation matrix method.

In recent years, the structure-borne sound analysis and control of flexible structures and cabins of marine-structures and aeronautical crafts are becoming an important topic. The use of vibrational power flow in a problem of this type is very valuable. An attempt to decrease the radiation or vibration in a structure by reducing only the force or velocity amplitude and not considering the relative phase angle may not necessarily be successful, but an improvement may be ensured by decreasing the net vibrational power applied to a structure. The premise of the effort proposed here is that damage to a structure will correspond in some way to changes, though small, in the structure's damping and stiffness properties and so the vibrational power flow is influenced by the changes of propagating waves. Li et al. [7–9] has researched the relations of the vibrational power flow, the position and the characteristic size of the damage in Euler beam structure and the circular plate structure.

The aim of this paper is to investigate the power flow characteristics of the Timoshenko beam with an open crack. By considering the crack as a rotational spring, the wave solutions of the perfect Timoshenko beam and cracked Timoshenko are deduced. The comparison of perfect beam's power flow and cracked beam's power flow characteristics are performed. The relation between the power flow characteristics of the cracked Timoshenko beam and the crack's characteristics are discussed in detail.

2. Flexural vibration of Timoshenko beam

By applying Hamilton's principle, the coupled differential equations for transverse vibration of a uniform Timoshenko beam with constant cross-section are given by [10]:

$$\rho A_s \ddot{y} - GkA_s(y'' - \phi') = f(x,t), \tag{1}$$

$$\rho I \ddot{\phi} - EI\phi'' - GkA_s(y' - \phi) = 0, \tag{2}$$

where a dot indicates partial differentiation with respect to time, and a prime indicates partial differentiation with respect to x. y is the transverse deflection of the center line of the beam, ϕ the slope of the deflection curve due to bending deformation, ρ the mass density, A_s the area of the cross-section, E the modulus of elasticity, I the moment of inertia, G the shear modulus, k the Timoshenko beam shear coefficient, which is a function of the Poisson ratio v and the shape of the cross-section [11].

By eliminating ϕ form Eqs. (1) and (2) one can get the equation about the transverse displacement y. So the Timoshenko beam equation of free vibration can be written as:

$$EIy^{iv} + \rho A_s \ddot{y} - \rho I(1 + E/kG)\ddot{y}'' + (\rho^2 I/kG)\ddot{\ddot{y}} = 0, \tag{3}$$

$$EI\phi^{iv} + \rho A_s \ddot{\phi} - \rho I(1 + E/kG)\ddot{\phi}'' + (\rho^2 I/kG)\ddot{\ddot{\phi}} = 0. \tag{4}$$

For harmonic motion, y and ϕ can be written as

$$y(x,t) = Y(x)e^{i\omega t}, \tag{5}$$

$$\phi(x,t) = \Phi(x)e^{i\omega t}, \tag{6}$$

where $i = \sqrt{-1}$, ω is the angular frequency. Substituting Eq. (5) into Eq. (3), one can get

$$Y^{iv} + (m+n)Y'' + (mn - p)Y = 0, \tag{7}$$

where $m = \rho\omega^2/E$, $n = \rho\omega^2/kG$, $p = \rho A_s\omega^2/EI$.

Define two wavenumbers

$$k_1 = \sqrt{\sqrt{\left(\frac{m-n}{2}\right)^2 + p} - \frac{m+n}{2}}, \quad k_2 = \sqrt{\sqrt{\left(\frac{m-n}{2}\right)^2 + p} + \frac{m+n}{2}}, \tag{8}$$

the general solution of Eq. (7) is of the form:

$$Y(x) = Ae^{k_1 x} + Be^{-k_1 x} + Ce^{ik_2 x} + De^{-ik_2 x}. \tag{9}$$

Similarly, for the slope of the deflection curve, one can easily derive that:

$$\Phi(x) = Aq_1 e^{k_1 x} - Bq_1 e^{-k_1 x} - iCq_2 e^{ik_2 x} + iDq_2 e^{-ik_2 x}, \tag{10}$$

where $q_1 = (k_3^2 + k_1^2)/k_1$, $q_2 = (k_3^2 - k_2^2)/k_2$, $k_3 = \sqrt{n}$, the constant coefficients A,B,C,D can be determined by the boundary conditions of the Timoshenko beam.

From Eq. (8), it can be seen that k_2 is always real and positive, while k_1 may be real, zero or imaginary, depending on the value of ω. This leads to the appearance of two spectra in the frequency domain. When $k_1 = 0$, there exists a critical frequency ω_c, which can be written as

$$\omega_c = \sqrt{\frac{kGA_s}{\rho I}} = \frac{1}{r}\sqrt{\frac{kG}{\rho}}, \tag{11}$$

where r is the radius of gyration.

By substituting Eq. (11) into Eq. (8), the critical wavenumbers are

$$k_{1c} = 0, \quad k_{2c} = \frac{1}{r}\sqrt{\frac{kG}{E} + 1}.$$

If $\omega < \omega_c$, k_1 is real. It can be seen from Eqs. (9) and (10) that one imaginary pair and two real and symmetric wave components occur. The solution leads to two pair of propagating and evanescent waves.

If $\omega > \omega_c$, k_1 is imaginary. The solutions are two pairs of waves, propagating at two different speeds.

In this paper, the concerned frequencies are limited within the first spectrum of frequencies. So $\omega < \omega_c$ and k_1 is real.

The bending moment M and shear force Q transmitted through an arbitrary section of the beam are, respectively,

$$M(x) = EI\Phi', \quad Q(x) = GA_s k(Y' - \Phi). \tag{12}$$

Considering an infinite Timoshenko beam where the positive wave motion along x direction, one can get $A = C = 0$, the solution of the beam can be simplified as

$$Y(x) = Be^{-k_1 x} + De^{-ik_2 x}, \quad \Phi(x) = -Bq_1 e^{-k_1 x} + iDq_2 e^{-ik_2 x}.$$

If a concentrated harmonic force $F = F_0 e^{i\omega t}$ is applied at the position of $x = 0$, the boundary conditions are

$$\text{at } x = 0 : \Phi(x) = 0, \quad Q(x) = F_0/2. \tag{13}$$

By substituting the expressions of $Y(x)$ and $\Phi(x)$ into the boundary conditions, one can get:

$$\begin{aligned} -Bq_1 + iDq_2 &= 0, \\ (-k_1 + q_1)B + (-ik_2 - iq_2)D &= \frac{F_0}{2GkA_s}. \end{aligned} \tag{14}$$

The values of B and D can be deduced from the above equations:

$$B = \frac{-F_0}{2GkA_s}\frac{q_2}{k_1 q_2 + k_2 q_1}, \quad D = \frac{iF_0}{2GkA_s}\frac{q_1}{k_1 q_2 + k_2 q_1}. \tag{15}$$

So the positive wave solutions of a perfect infinite Timoshenko beam are deduced.

3. Analysis of the cracked beam

An infinite Timoshenko beam with uniform circular cross-section is considered as shown in Fig. 1. The beam has a diameter $D = 2R$ and a transverse surface crack of depth a, which is located at distant c from the position of $x = 0$. This research assumes the crack is on surface and remains open to avoid nonlinear problems. Because bending moment is dominant in the beam, all other coupling terms may be neglected, only the bending flexibility is considered here [2], as can be seen from Fig. 2. For structural mass, the effects of damage are usually very small and often can be neglected. Thus the crack is represented by a rotational spring. Because the concentrated harmonic force $F = F_0 e^{i\omega t}$ is applied at the position of $x = 0$, the cracked beam can be divided into three segments: the semi-infinite region of $x \leqslant 0$, the finite part of $0 \leqslant x \leqslant c$, the semi-infinite region of $x \geqslant c$, and the last two parts are connected by the rotational spring.

The local flexibility of the crack for bending moment in the ξ direction is obtained as [12]:

$$C' = \frac{\partial^2}{\partial M^2} \int_{-b}^{b} \int_{0}^{\eta} \frac{(1-\nu^2)K_1^2}{E} \, d\eta \, d\xi, \tag{16}$$

where the stress factor intensity

$$K_I = (4M/\pi R^4)\sqrt{R^2 - \xi^2}\sqrt{\pi\eta} F_2(\eta/h).$$

So

$$C' = \frac{1-\nu^2}{E} \int_{-b}^{b} \int_{0}^{\eta} \frac{32}{\pi^2 R^8} (R^2 - \xi^2)\pi\eta F_2^2(\eta/h) \, d\eta \, d\xi. \tag{17}$$

The geometric function $F_2(\eta/h)$ is [13]:

$$F_2(\eta/h) = \sqrt{\frac{2h}{\pi\eta} \tan\left(\frac{\pi\eta}{2h}\right)} \frac{0.923 + 0.199(1 - \sin(\pi\eta/2h))^4}{\cos(\pi\eta/2h)}, \tag{18}$$

h being the local height, $h = 2\sqrt{R^2 - \xi^2}$. The accuracy of this geometric function is better than 0.5% for any η/h [13].

The solutions of the three regions can be written, respectively as,

$$\begin{aligned} Y_1(x) &= A_1 e^{k_1 x} + B_1 e^{-k_1 x} + C_1 e^{ik_2 x} + D_1 e^{-ik_2 x}, \\ \Phi_1(x) &= A_1 q_1 e^{k_1 x} - B_1 q_1 e^{-k_1 x} - iC_1 q_2 e^{ik_2 x} + iD_1 q_2 e^{-ik_2 x}, \end{aligned} \quad x \leqslant 0, \tag{19}$$

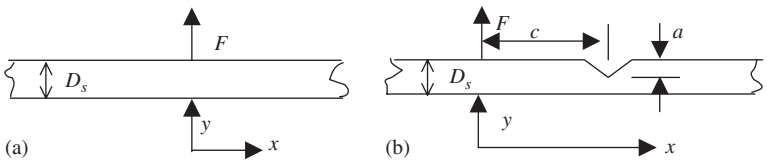

Fig. 1. (a) Infinite perfect beam, (b) infinite cracked beam.

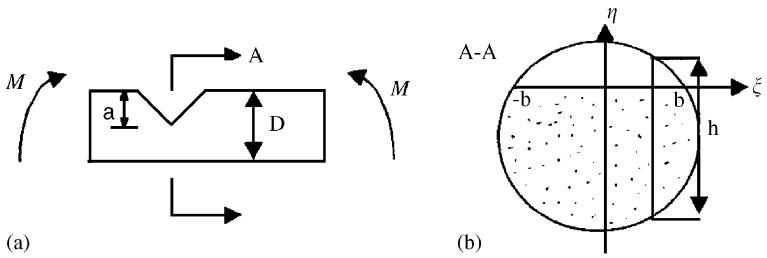

Fig. 2. (a) Model of cracked beam, (b) cross section of the crack.

$$\begin{aligned} Y_2(x) &= A_2 e^{k_1 x} + B_2 e^{-k_1 x} + C_2 e^{ik_2 x} + D_2 e^{-ik_2 x}, \\ \Phi_2(x) &= A_2 q_1 e^{k_1 x} - B_2 q_1 e^{-k_1 x} - iC_2 q_2 e^{ik_2 x} + iD_2 q_2 e^{-ik_2 x}, \end{aligned} \quad 0 \leqslant x \leqslant c, \tag{20}$$

$$\begin{aligned} Y_3(x) &= A_3 e^{k_1 (x-c)} + B_3 e^{-k_1 (x-c)} + C_3 e^{ik_2 (x-c)} + D_3 e^{-ik_2 (x-c)}, \\ \Phi_3(x) &= A_3 q_1 e^{k_1 (x-c)} - B_3 q_1 e^{-k_1 (x-c)} - iC_3 q_2 e^{ik_2 (x-c)} + iD_3 q_2 e^{-ik_2 (x-c)}, \end{aligned} \quad x \geqslant c. \tag{21}$$

For the semi-infinite region of $x \leqslant 0$, only negative wave exists and reflected wave vanishes, so $B_1 = 0$, $D_1 = 0$. Similarly, for the semi-infinite region of $x \geqslant c$, only positive wave exists and reflected wave vanishes, $A_3 = 0$, $C_3 = 0$. Thus there are eight unknown coefficients in the above equations.

There are continuous conditions at $x = 0$:

$$Y_1 = Y_2, \quad \Phi_1 = \Phi_2, \quad M_1 = M_2, \quad -Q_1 + Q_2 = F_0. \tag{22}$$

At $x = c$, conditions can be introduced which impose continuity of displacement, bending moment and shear force at the crack location:

$$Y_2 = Y_3, \quad M_2 = M_3, \quad Q_2 = Q_3. \tag{23}$$

The crack is supposed to give rise to a jump in slope [3]. The transition can be written in the following form:

$$\Phi_2 + C' EI \Phi_2' = \Phi_3. \tag{24}$$

Substitution of the expressions of $Y_j(x), \Phi_j(x)$ $(j = 1, 2, 3)$ into the above eight equations yields the characteristic equations:

$$\begin{bmatrix} 1 & 1 & -1 & -1 & -1 & -1 & 0 & 0 \\ q_1 & -iq_2 & -q_1 & q_1 & iq_2 & -iq_2 & 0 & 0 \\ t_1 & t_2 & -t_1 & -t_1 & -t_2 & -t_2 & 0 & 0 \\ t_3 & -it_4 & -t_3 & t_3 & it_4 & -it_4 & 0 & 0 \\ 0 & 0 & e^{t_5} & e^{-t_5} & e^{it_6} & e^{-it_6} & -1 & -1 \\ 0 & 0 & t_1 e^{t_5} & t_1 e^{-t_5} & t_2 e^{it_6} & t_2 e^{-it_6} & -t_1 & -t_2 \\ 0 & 0 & -t_3 e^{t_5} & t_3 e^{-t_5} & it_4 e^{it_6} & -it_4 e^{-it_6} & -t_3 & it_4 \\ 0 & 0 & (t_7 + q_1) e^{t_5} & (t_7 - q_1) e^{-t_5} & (t_8 - iq_2) e^{it_6} & (t_8 + iq_2) e^{-it_6} & q_1 & -iq_2 \end{bmatrix} \begin{bmatrix} A_1 \\ C_1 \\ A_2 \\ B_2 \\ C_2 \\ D_2 \\ B_3 \\ D_3 \end{bmatrix} = \begin{Bmatrix} 0 \\ 0 \\ 0 \\ \frac{F_0}{GA_s k} \\ 0 \\ 0 \\ 0 \\ 0 \end{Bmatrix},$$

where $t_1 = q_1 k_1$, $t_2 = q_2 k_2$, $t_3 = -k_1 + q_1$, $t_4 = k_2 + q_2$, $t_5 = k_1 c$, $t_6 = k_2 c$, $t_7 = -k_1 C' EI$, $t_8 = q_2 k_2 C' EI$.

So the expressions of A_j, B_j, C_j, D_j $(j = 1, 2, 3)$ can be derived from the characteristic equations.

4. Flexural power flow in Timoshenko beam

When the beam structures vibrate in the state of single frequency, the structural power flow input by the external force propagates to far field continuously. The time-averaged power flow by the point force is [14]

$$P_{\text{in}} = \frac{1}{2} \text{Re}(-i\omega F_0 Y^*) = \frac{1}{2} |F_0|^2 \text{Re}(\bar{M}) = \frac{1}{2} |Y_0|^2 \text{Re}(\bar{Z}), \tag{25}$$

where Re(*) expresses the real part of a complex value, an asterisk denotes the complex conjugate, $\bar{M}, \bar{Z}$, are the force point mobility and impedance, respectively.

Substituting the expression of Y into the above equation, the input power flow of the perfect Timoshenko beam is

$$P_{\text{in}} = \frac{1}{2} F_0 \omega \, \text{Re}\{-i(Be^{-k_1 x} + De^{-ik_2 x})^*\} = \frac{1}{2} F_0 \omega \, \text{Re}\{-i(Be^{-k_1 x})^*\} + \frac{1}{2} F_0 \omega \, \text{Re}\{-i(De^{-ik_2 x})^*\}.$$

When $\omega<\omega_c$, k_1 and k_2 are both real, q_1 and q_2 are real as well. So B is real, D is purely imaginary. Considering $x=0$, the input power flow can be written as

$$P_{\text{in}}=\frac{1}{2}F_0\omega\,\text{Re}\{-\text{i}D^*\}=\frac{1}{2}F_0\omega\,\text{Re}\left\{-\text{i}\frac{-\text{i}F_0}{2GkA_s}\frac{q_1}{k_1q_2+k_2q_1}\right\}=\frac{1}{4}\frac{F_0^2\omega}{GkA_s}\frac{q_1}{k_1q_2+k_2q_1}.$$

Substituting the expressions of q_1, q_2 into the above equation, we can get

$$P_{\text{in}}=\frac{F_0^2}{4\rho\omega A_s}\frac{k_2(k_1^2+k_3^2)}{k_1^2+k_2^2}. \tag{26}$$

Similarly, the input power flow of cracked Timoshenko beam can also be calculated.

The transmitted power flow along a beam has two terms: the bending moment times the angular velocity and the shear force times the velocity. For harmonic analysis, the force and the velocity are described as complex quantities and as functions of frequency. The flexural velocity and angular velocity are, respectively,

$$\dot{y}(x,t)=\text{i}\omega Y(x),\quad \dot{\phi}(x,t)=\text{i}\omega\Phi(x).$$

The transmitted power flow at any point along a Timoshenko beam is then given by

$$P_{\text{tr}}=\frac{1}{2}\,\text{Re}(-\text{i}\omega M\Phi^*)+\frac{1}{2}\,\text{Re}(-\text{i}\omega QY^*). \tag{27}$$

Because the shear force can also be written as

$$Q(x)=GkA_s(Y'-\Phi)=-EI\Phi''+\rho I\ddot{\Phi},$$

the transmitted power flow can be expressed as following form:

$$P_{\text{tr}}=\frac{1}{2}\,\text{Re}\{-\text{i}\omega(EI\Phi')\Phi^*-\text{i}\omega(-EI\Phi''-\omega^2\rho I\Phi)Y^*)\}. \tag{28}$$

Based on above analysis, the input power flow and transmitted power flow of the cracked Timoshenko beam are functions of position and the characteristic size of the crack. The input power flow and the transmitted power flow in the cracked beam can be easily measured in practical engineering. The power flow input into the beam can be directly measured with an impedance head [14]. The bending wave power flow carried by internal forces $Q(x)$ and $M(x)$ in far field can be measured using a two-accelerometer array or alternatively using a biaxial accelerometer [15,16]. However, the measurement of power flow in Refs. [15,16] is based on Euler beam theory. In Ref. [17], for the measurement of bending wave power flow in one-dimensional structures, the error caused by the omission of shear force and rotating inertia error at high frequencies was analyzed. In addition, the modified measurement formulas based on Timoshenko beam theory were given. In this way the bending wave power flow in the cracked Timoshenko beam can be measured as well by using a two-accelerometer array. So the crack may be diagnosed by comparing the vibrational power flow of the cracked Timoshenko beam with that of the perfect Timoshenko beam.

5. Numerical results and discussions

In this paper, an undamped infinite steel beam with $R=2.5\,\text{cm}$, modulus of elasticity $E=200\,\text{GPa}$, Poisson's ratio $v=0.3$ and mass density $\rho=7800\,\text{kg/m}^3$ is considered. The critical frequency $f_c=\omega_c/2\pi=\sqrt{kGA_s/4\pi^2\rho I}=3.76\times10^4$ Hz, which is very high. There is only a crack on its surface, if the crack depth is a, the crack width b is $\sqrt{R^2-(R-a)^2}$. For cracked beam structure, the crack is situated at different positions c and the crack depth a is a variable as well.

Fig. 3 (a) and (b) show how the input power flows of perfect and cracked Timoshenko beam vary over the frequency range when changing the relative crack depth a/D and the relative location C/D, respectively. The coordinate of X-axis is f(Hz), and the coordinate of Y-axis is $\log_{10}(P_{\text{in}}/F_0^2)$ (dB). The frequency range is from 1 to 2000 Hz. From Fig. 3 it can be seen that both the input power flow of perfect beam and that of cracked beam decrease with the increase of the frequency. The input power flow of cracked Timoshenko beam fluctuates around

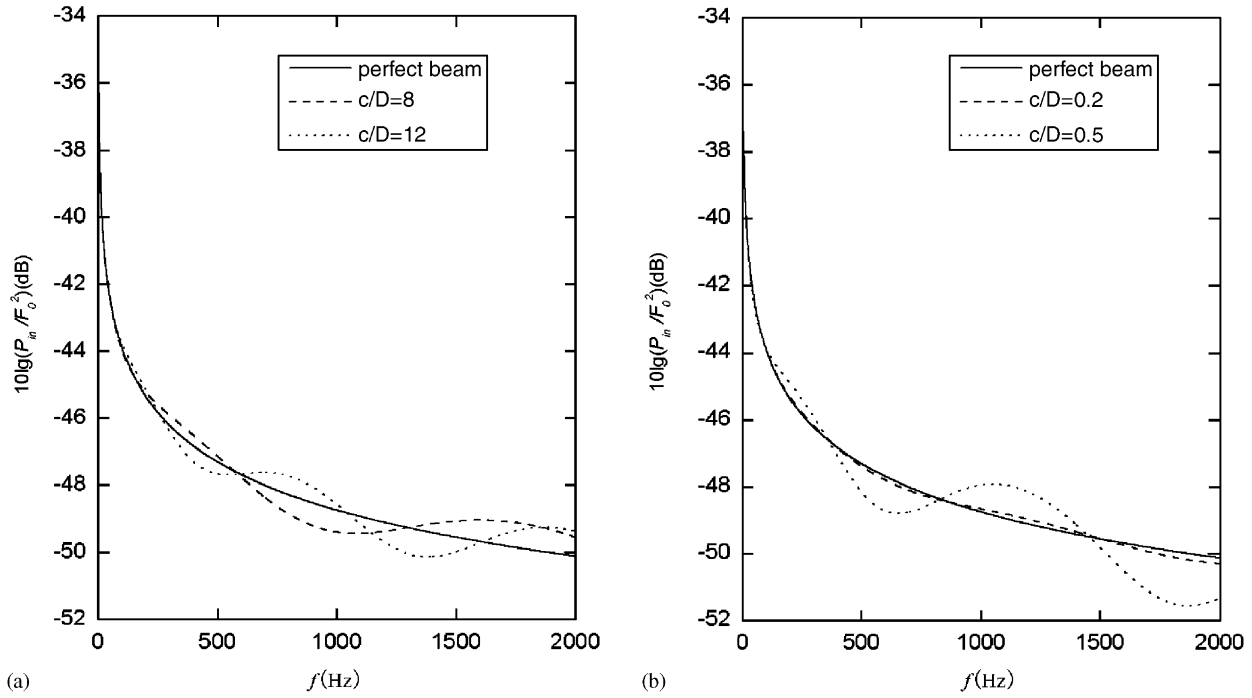

Fig. 3. Input power flow level of cracked beam. (a) $a/D = 0.4$, (b) $c/D = 10$.

that of the pefect beam and the amplitude of fluctuation increases when the frequency increases. It can be seen from Fig. 3(a) that the input power flow curve fluctuates more and more quickly over the same frequency range with increasing distance between the acting point and the cracked point. In Fig. 3(b), the degree of fluctuation increases over the same frequency range when the relative depth of the crack changes from 0.2 to 0.5.

In Fig. 4, the coordinate of X-axis is the relative location c/D. When only changing crack depth and keeping driving frequency constant, the shape of the input power flow curves is almost sinusoidal, though a/D is different. The input power flow of the cracked beam fluctuates around that of the perfect beam. The wavelength of different curves is identical, but the amplitude increases with increasing the depth of crack. It can be seen from Fig. 4(b) that the wavelength of input power flow curve is shorter with increasing driving frequency when the depth of the crack keeps constant. Moreover, the input power flow level decreases when the driving frequency increases.

Besides the input power flow of Timoshenko beam, the transmitted power flows of perfect and cracked Timoshenko beam are also considered. The calculated results reveal that for perfect beam the transmitted power flows along positive direction $x \geqslant 0$ and along negative direction $x \leqslant 0$ keep constant and equivalent under the same frequency except the near-field regions near acting point. The transmitted power flow along one direction is half of the input power flow under the same driving frequency. For cracked Timoshenko beam, when the driving frequency is fixed, the transmitted power flows along the two directions also keep constant except the near-field regions near acting point and cracked point, but the two constants are different. As damping is not considered, the transmitted power flows do not change along the propagating direction in the far-field regions.

The ratio of transmitted power flow along positive direction to the input power flow of cracked beam (defined by $P_{\mathrm{tr}}/P_{\mathrm{in}}$) is shown in Figs. 5(a) and (b) when changing c/D and changing a/D, respectively. The straight line is the transmitted power flow ratio curve of the perfect beam, which denotes the input power flow is divided two equal parts propagating along positive and negative directions, respectively. For the cracked beam, the ratios of the transmitted power flows along both sides of the acting point to the input power flow are not equal, and the curve fluctuates around the straight line $P_{\mathrm{tr}}/P_{\mathrm{in}} = 1/2$. However, the sum of the transmitted power flows along both sides of the driving point is equal to the input power flow. It also can be seen that the

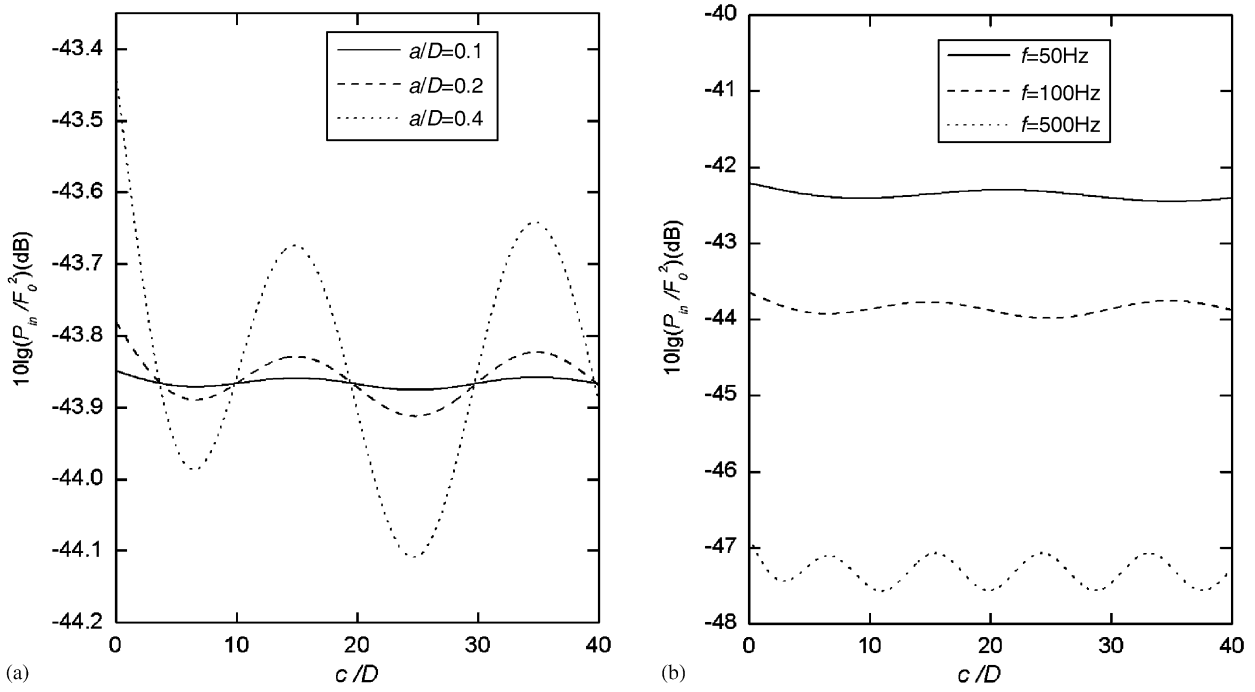

Fig. 4. Input power flow level of cracked beam. (a) $f = 100\,\text{Hz}$, (b) $a/D = 0.3$.

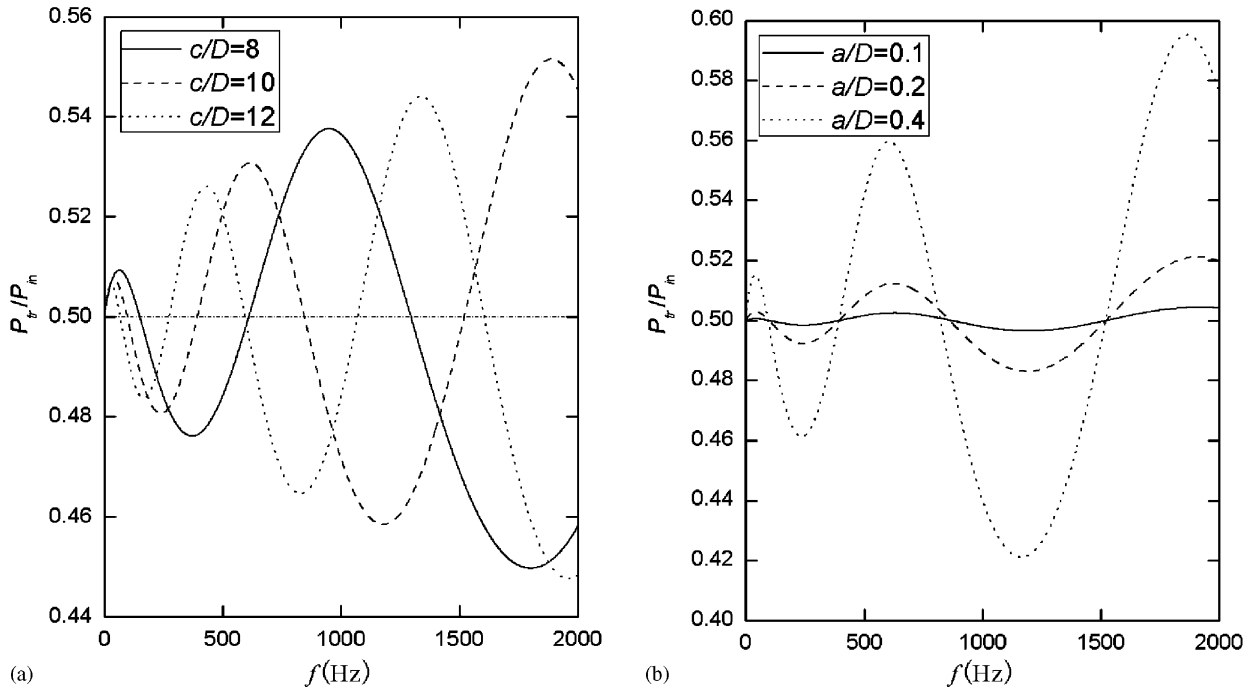

Fig. 5. Transmitted power flow ratio curves of cracked beam. (a) $a/D = 0.3$, (b) $c/D = 10$.

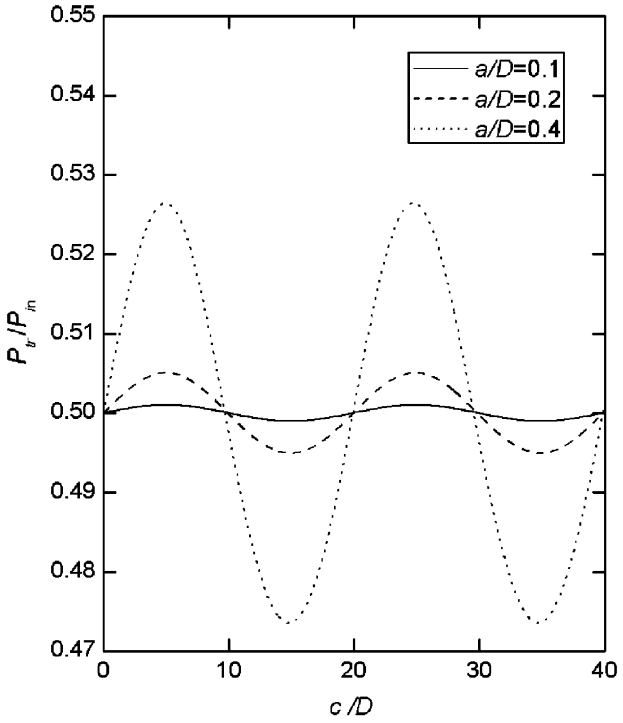

Fig. 6. Transmitted power flow ratio curves of cracked beam ($f = 100$ Hz).

characteristics of the transmitted power flow ratio curves are similar to those of the input power flow curves when increasing c/D and a/D, respectively. When $c = 0$, $P_{tr}/P_{in} = 0.5$, which implies that the transmitted power flows along both directions are equal when the acting point locates at the crack point, like the case of perfect beam. Fig. 6 shows the ratio of transmitted power flow versus the relative crack location. The curves are all sinusoidal. The wavelengths of the curves are almost identical for different relative crack depth, but the amplitude increases with increasing crack depth.

From Figs. 3 and 5, it can be found that the changes of input power flow and transmitted power flow ratio of cracked beam versus those of perfect beam are more evident when the driving frequency is higher. That is to say, the power flow characteristics in the beam are more sensitive to crack's parameters at higher frequencies. Thus the acquirement of the power flow at high frequencies will be more effective. However, it is obvious that the omission of shear deformation and rotating inertia results in a large bias error at high frequencies when calculating the flexural power flow in one-dimensional structures [17]. Consequently, it is necessary to adopt Timoshenko beam theory to calculate the flexural power flow at high frequencies.

In Fig. 7, the cracked beam's input power flow levels calculated by both Euler beam theory and Timoshenko beam theory are plotted, the perfect beam's input power flow levels by using two theories being drawn likewise to compare with the cracked beam's results. From the figure it is clear that the cracked beam's input power flow level from Euler beam theory fluctuates around that of perfect beam from the same theory. The same results about cracked Euler beam can also be found in Ref. [9]. For both the perfect beam and cracked beam, the input power flow obtained from Euler beam theory are coincident with that from Timoshenko beam theory when the driving frequency is much smaller than the critical frequency, but the deviation between the two theories becomes very obvious with increasing driving frequency. For the cracked beam, it can be seen that the difference of the power flow levels between the two theories is bigger than 6 dB when $f/f_c = 0.4$. Therefore, for the accurate analysis of the cracked beam power flow characteristics at high frequencies, the consideration of Timoshenko beam theory in this paper is necessary and valuable.

When considering the structural damping, the complex elastic modulus E' may be introduced, where $E' = E(1 + i\eta)$, η is the damping loss factor. By substituting E' into the above equations of wave motion, the

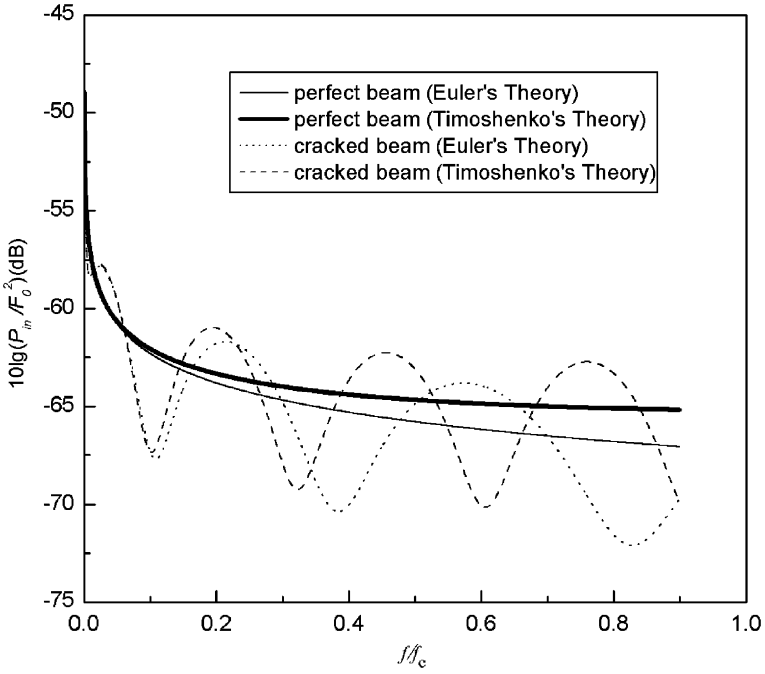

Fig. 7. Input power flow level of perfect beam and cracked beam using two theories.

solutions can be deduced as well. The numerical results indicate the relations between the power flow characteristics of the Timoshenko beam and the information of the crack (location and depth) are similar to those of undamped beam.

Based on above analysis, it can be found that the existence of the crack causes the change of flexural wave motion in the Timoshenko beam, and the numerical results demonstrate that vibrational power flow characteristics of the Timoshenko beam are close related to both the location and depth of the crack. Define the ratio of cracked Timoshenko beam's input power flow to uncracked beam's input power flow is the normalized input power flow. The contour lines of the normalized input power flow could be plotted in a figure from different combination of normalized crack location and depth under some specified frequencies via the analytical solutions above, the figure having the normalized crack location and depth as its axes. Fig. 8 shows the contours of normalized input power flow of cracked Timoshenko beam when driving frequency is 1000 Hz. In order to be clear and readable, only part of the contours are plotted and labeled. The 0.88 contour means the points on the curve have 88% input power compared to the uncracked beam. The location and depth corresponding to any point on the curve would become the possible crack location and depth. The contour lines from two different driving frequencies can be plotted together, and the intersection point would indicate the location and depth of the crack. When more than one intersection point is obtained from the merged figure, the contour from another driving frequency could be used to uniquely obtain the correct point, which would indicate the crack location and depth.

For example, assume that certain crack exists in the Timoshenko beam. The normalized input power flow of the cracked beam is 0.925 when the driving frequency is 1000 Hz and is 0.938 with frequency of 800 Hz. Thus the solid contour with the value of 0.925 under 1000 Hz can be plotted in Fig. 9. The dash contour with the value of 0.938 under 800 Hz is plotted in the same figure. It can be seen that there are two intersection points for these two contours. So the dot contour with the value of 0.963 under 1200 Hz can be used to uniquely obtain the final point, as can be seen from Fig. 9. The final point indicates that the relative depth is 0.3 and the relative position 8 in this case. Therefore, according to the contour diagram of different frequencies, the crack's position and depth of Timoshenko beam may be detected. Besides the input power flow, the contour lines of transmitted power flow can also be constructed to identify the crack.

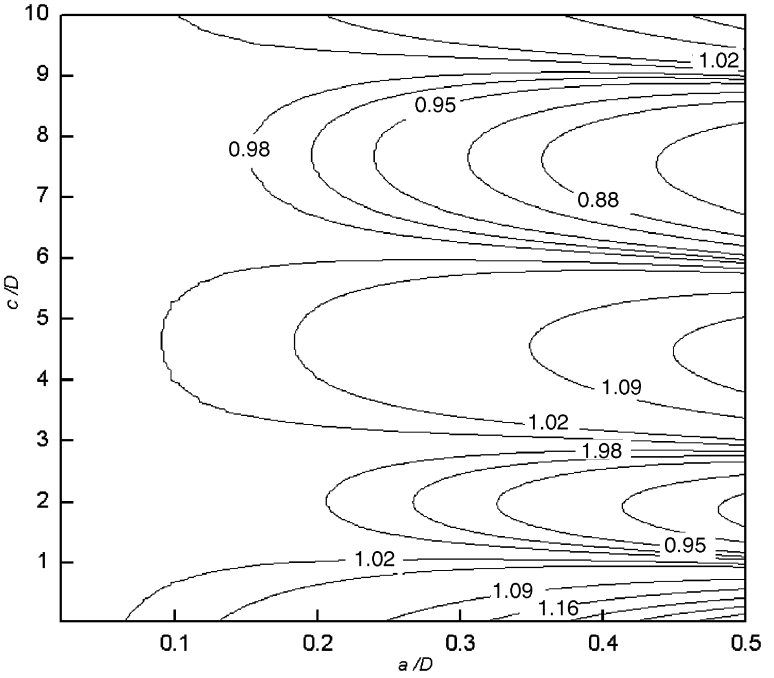

Fig. 8. Contours of normalized input power flow with driving frequency of 1000 Hz.

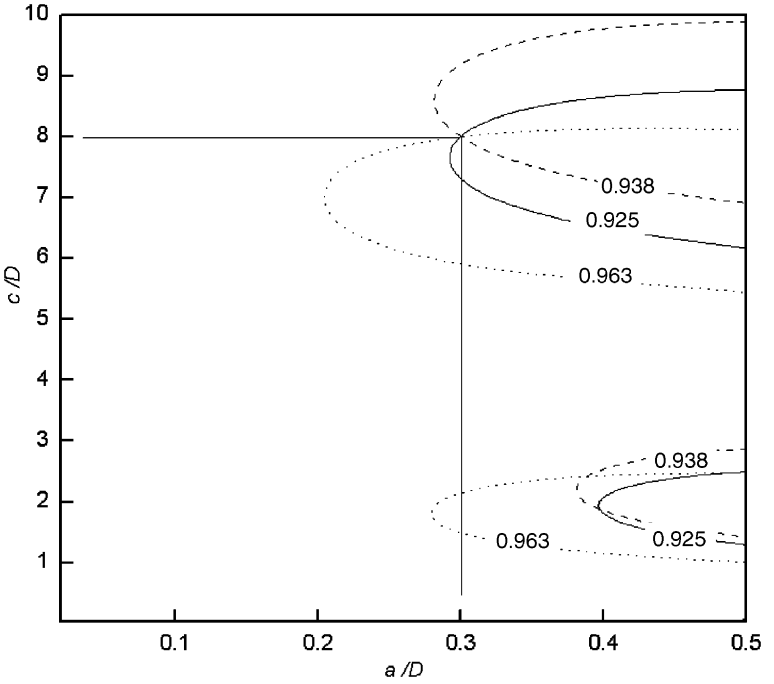

Fig. 9. Crack identification by normalized input power flow contours from three different driving frequency.

6. Conclusion

This paper presented an approach to analyze the vibrational power flow characteristics of cracked Timoshenko beam structures. The case of an infinite Timoshenko beam with an open crack is considered. The

wave motion and vibrational power flow characteristics under point driving force are researched. Changes in input and transmitted power flows with respect to the crack location and crack ratio are obtained. The results show that the vibrational power flow characteristics of cracked Timoshenko beam are extraordinary related to the crack location and crack depth, especially at high frequencies. Contour lines of input power flow under different frequencies are constructed to identify the crack position and depth.

The research in this paper provides guidance to crack detection by measuring the vibrational power flow of cracked Timoshenko beam. It should be pointed out that the power flow characteristics are not very sensitive to small cracks ($a/D<0.1$), so the method lacks accuracy for some small cracks. The application of the method may suit the moderate cracks. As a global crack detection method, it is believed that this method provides a simple and useful tool to detect a crack without the access of the whole Timoshenko beam structure. Further work will be done to investigate the cracked finite Timoshenko beam's power flow characteristics and diagnose the crack based on the power flow analysis presented in this paper.

Acknowledgments

The authors are grateful for the financial assistance provided by National Natural Science Foundation of China (Contract No. 50375059).

References

[1] H.T. Banks, D.J. Inman, D.J. Leo, Y. Wang, An experimentally validated damage detection theory in smart structures, *Journal of Sound and Vibration* 191 (5) (1996) 859–880.
[2] G. Gounaris, A. Dimarogonas, Finite element of a cracked prismatic beam for structural analysis, *Computers and Structures* 28 (3) (1988) 309–313.
[3] P.F. Rizos, N. Aspragathos, A.D. Dimarogonas, Identification of crack location and magnitude in a cantilever beam from the vibration modes, *Journal of Sound and Vibration* 138 (3) (1990) 381–388.
[4] S.P. Lele, S.K. Maiti, Modelling of transverse vibration of short beams for crack detection and measurement of crack extension, *Journal of Sound and Vibration* 257 (3) (2002) 559–583.
[5] M. Krawczuk, M. Palacz, W. Ostachowicz, The dynamic analysis of a cracked Timoshenko beam by the spectral element method, *Journal of Sound and Vibration* 264 (5) (2003) 1139–1153.
[6] J. Tian, Z. Li, X. Su, Crack detection in beams by wavelet analysis of transient flexural waves, *Journal of Sound and Vibration* 261 (4) (2003) 715–727.
[7] T.Y. Li, W.H. Zhang, T.G. Liu, Vibrational power flow analysis of damaged beam structures, *Journal of Sound and Vibration* 242 (1) (2001) 59–68.
[8] T.Y. Li, J.X. Liu, T. Zhang, Vibrational power flow characteristics of circular plate structures with peripheral surface crack, *Journal of Sound and Vibration* 276 (3–5) (2004) 1081–1091.
[9] T.Y. Li, T. Zhang, J.X. Liu, W.H. Zhang, Vibrational wave analysis of infinite damaged beams using structure-borne power flow, *Applied Acoustics* 65 (1) (2004) 91–100.
[10] R.R. Craig, *Structural Dynamics:An Introduction to Computer Methods*, Wiley, New York, NY, 1981.
[11] G.R. Cowper, The shear coefficient in Timoshenko's beam theory, *Journal of Applied Mechanics* (1966) 335–340.
[12] A.D. Dimarogonas, C.A. Papadopoulos, Vibration of cracked shafts in bending, *Journal of Sound and Vibration* 91 (4) (1983) 583–593.
[13] H. Tada, P.C. Paris, G.R. Irwin, *The Stress Analysis of Cracks Handbook*, Del Research Corporation, Hellertown, PA, 1973.
[14] R.J. Pinnington, R.G. White, Power flow through machine isolators to resonant and non-resonant beams, *Journal of Sound and Vibration* 75 (2) (1981) 179–197.
[15] J.W. Verheij, Cross-spectral density method for measuring structure borne power flow on beams and pipes, *Journal of Sound and Vibration* 70 (1) (1980) 133–139.
[16] D.U. Noiseux, Measurement of power flow in uniform beams and plates, *Journal of the Acoustical Society of America* 47 (1970) 238–247.
[17] R.S. Ming, R.J.M. Craik, Errors in the measurement of structure-borne power flow using two-accelerometer techniques, *Journal of Sound and Vibration* 204 (1) (1997) 59–71.